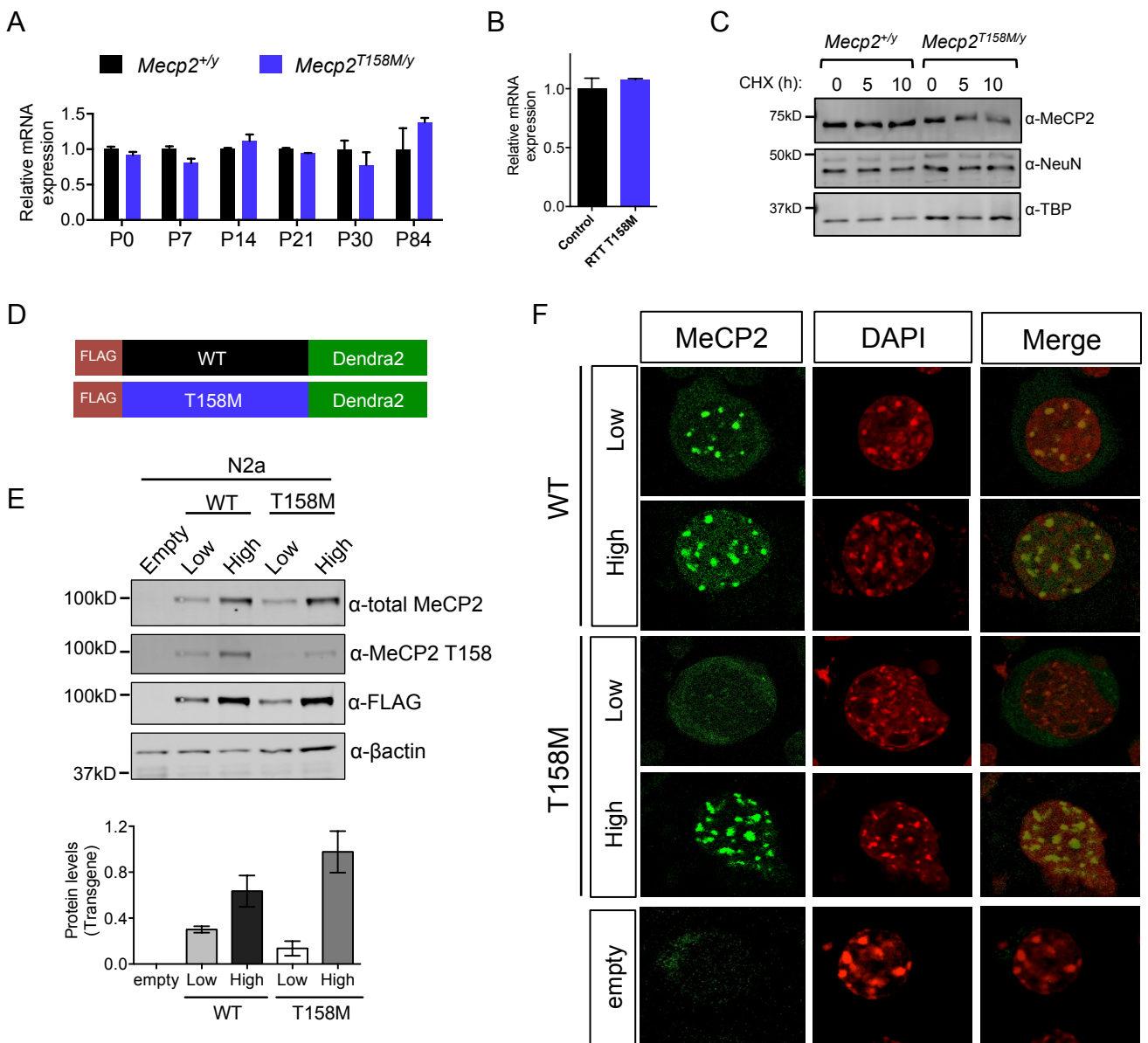
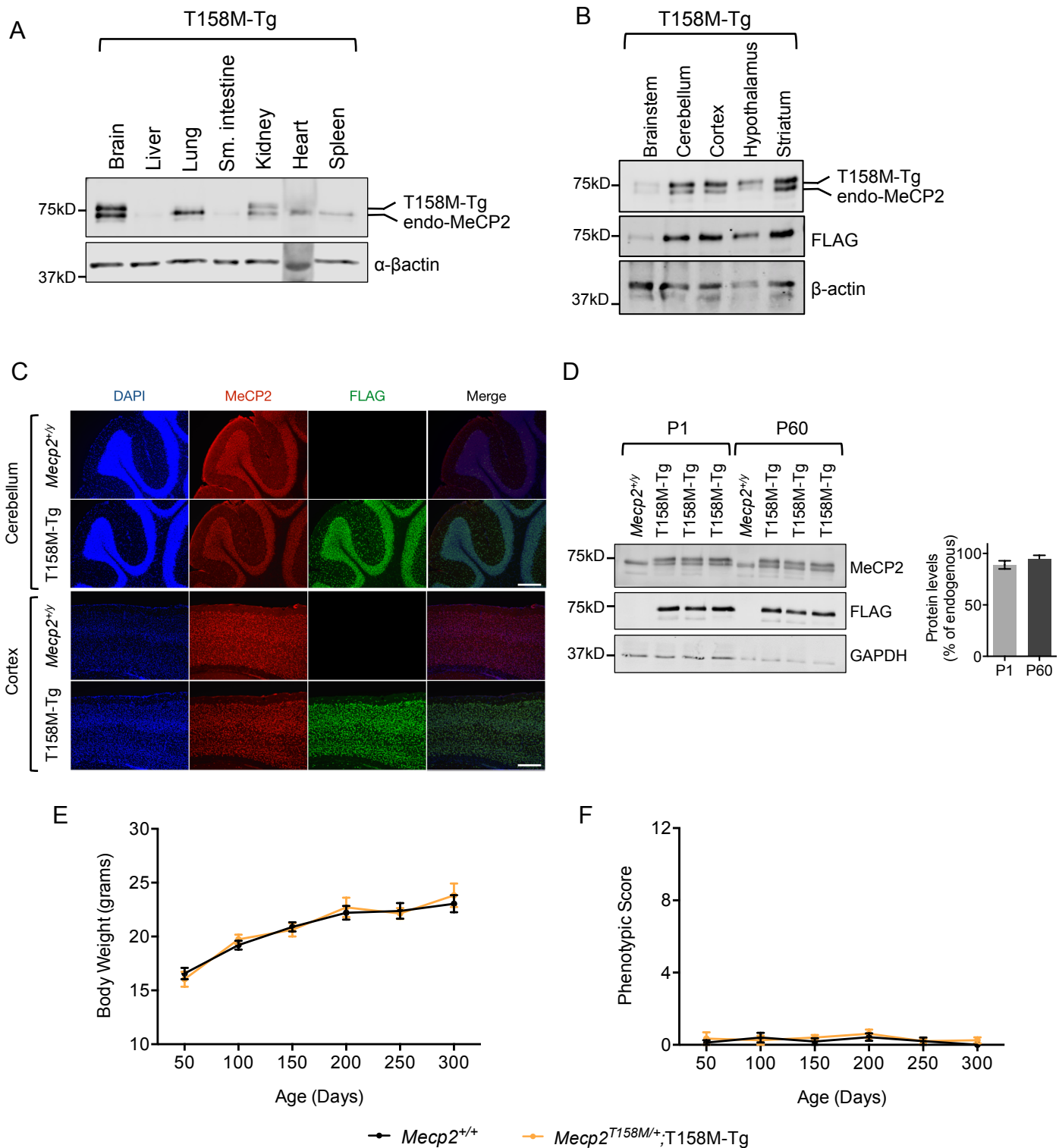


**Figure S1. Characterization of MeCP2 T158M knockin mice (A)** Schematic of the targeting strategy used to generate MeCP2 T158M knockin mice. MBD: methyl-CpG binding domain; TRD: transcription repression domain; Tavi: TEV protease cleavage and Avidin binding; NEO: Neomycin cassette. **(B)** Sequencing chromatogram confirming that codon 158 was mutated from ACG (threonine) to ATG (methionine) in *Mecp2*<sup>T158M/+</sup> animals. The asterisk represents the incorporation of a silent mutation in *Mecp2*<sup>T158M/+</sup> animals. **(C)** Western blot of whole brain nuclear lysates from *Mecp2*<sup>+/-</sup> and *Mecp2*<sup>T158M/+</sup> animals at P0. Blot was probed with an antibody recognizing total MeCP2, a site-specific antibody recognizing MeCP2 T158, and H3.



**Figure S2. Characterization of MeCP2 T158M knockin mice and tagged MeCP2- and MeCP2 T158M-expressing N2a cell lines.** (A) *Mecp2* mRNA expression in whole brain from *Mecp2*<sup>T158M/y</sup> and *Mecp2*<sup>+/y</sup> animals during development ( $n = 3$  per genotype and age). (B) *MECP2* mRNA expression in fibroblasts derived from a female RTT patient carrying the T158M mutation (RTT T158M) as compared to an age-matched female control ( $n = 3$ ). (C) Western blot of nuclear extracts from P0 + 3 d *in vitro* cortical cultures from animals of the indicated genotype treated with vehicle (0) or 100ug/ml CHX for 5 and 10 h. Blot is probed with antibodies against MeCP2, NeuN, and TBP. (D) Schematic of the lentiviral constructs used to make stable N2a cell lines. FLAG and Dendra2 tags were inserted in-frame N- and C-terminal to MeCP2 cDNA, respectively. (E) High and low-expressing N2a cell lines as determined by western blot analysis of nuclear extracts, probed for total MeCP2, MeCP2 T158M, FLAG, and  $\beta$ -actin. *Bottom*, Quantification of the level of MeCP2 fusion protein in each cell line. Values were normalized to  $\beta$ -actin and the results are displayed as fold-change relative to the T158M High line. ( $n = 3 - 4$  biological replicates per cell line). (F) Immunofluorescence of FLAG-MeCP2-Dendra2 and FLAG-T158M-Dendra2 in high and low-expressing stably infected N2a cell lines. All error bars represent  $\pm$  s.e.m.



**Figure S3. Characterization of T158M-Tg mice.** (A) Western blot analysis of MeCP2 protein levels in various tissues in T158M-Tg animals. Levels of transgenic MeCP2 T158M protein are highest in brain and low in liver, lung, small intestine, kidney, heart, and spleen. (B) Widespread distribution of MeCP2 T158M transgenic protein throughout the brains of T158M-Tg animals as assessed by Western blot. (C) Staining with MeCP2 and FLAG antibodies in cerebellum and cortex in *Mecp2*<sup>+/y</sup> and *Mecp2*<sup>+/y</sup>;T158M-Tg littermates. Scale bar corresponds to 500  $\mu$ m. (D) Western blot depicting MeCP2 protein levels in whole brain from *Mecp2*<sup>+/y</sup>;T158M-Tg and *Mecp2*<sup>+/y</sup> animals at P1 and P60. Right, Quantification of T158M-Tg protein levels. Values were normalized to GAPDH and the results are displayed as percent of endogenous MeCP2 ( $n = 3$  per age). (E) Female body weight and (F) phenotypic scores of *Mecp2*<sup>+/y</sup>;T158M-Tg animals relative to *Mecp2*<sup>+/+</sup> littermates up to age P300 ( $n = 10$  per genotype and age). All error bars represent mean  $\pm$  s.e.m.

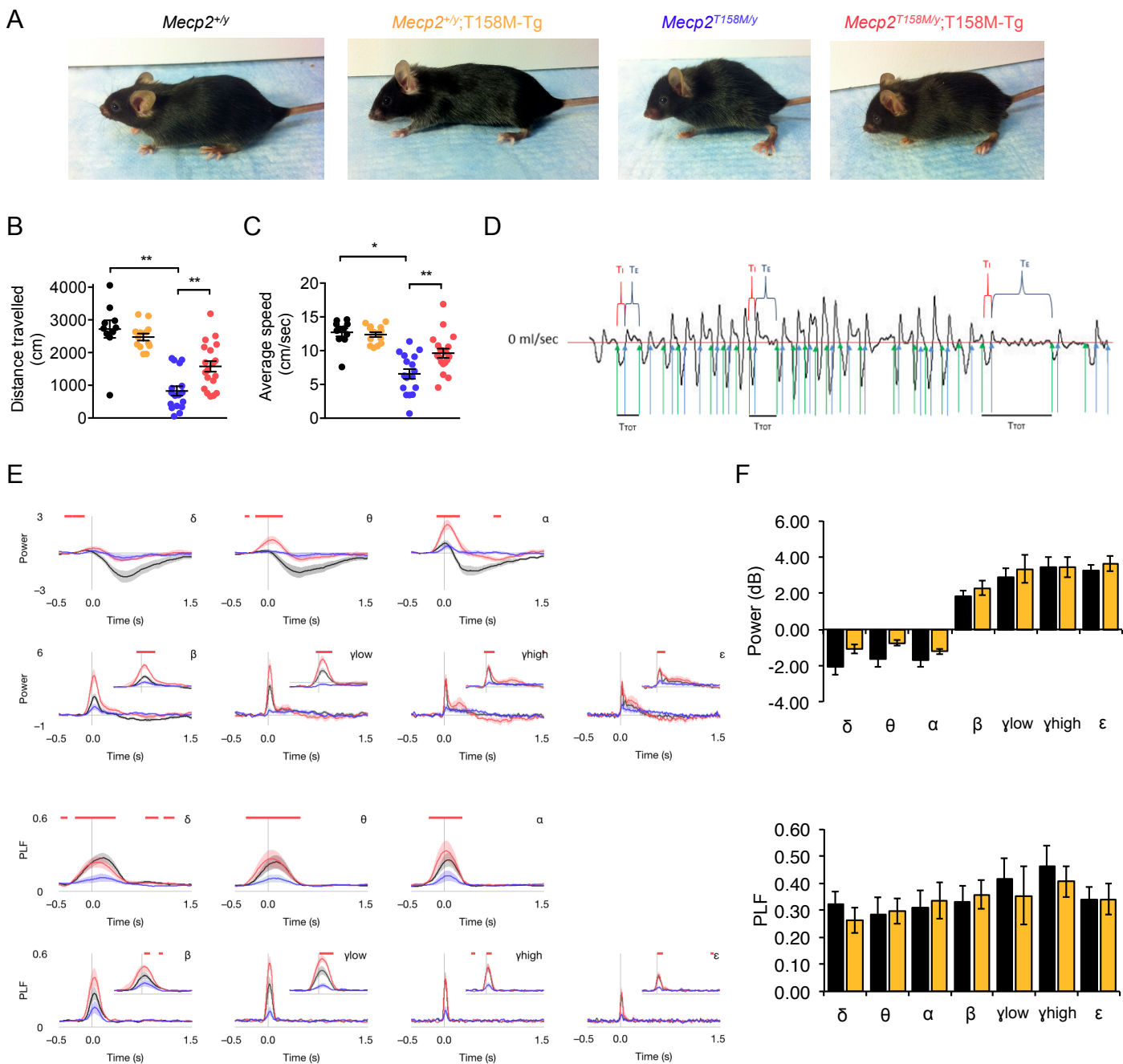


**Figure S4. An MeCP2 T158M transgene ameliorates RTT-like phenotypes in *Mecp2*<sup>T158M/y</sup> male mice.** (A) Representative images of *Mecp2*<sup>+/y</sup>, *Mecp2*<sup>+/y</sup>;T158M-Tg, *Mecp2*<sup>T158M/y</sup>, and *Mecp2*<sup>T158M/y</sup>;T158M-Tg animals at 10-weeks of age. (B) Distance travelled ( $n = 10, 13, 19, 17$  per genotype) and (C) Average speed ( $n = 11, 14, 18,$  and  $17$ ) of 10-week old mice in an open field. (D) Expanded respiratory tracing illustrating measurement and calculation of respiratory timing for the respiratory irregularity score based on flow vs. time. Total time for one breath (TTOT) is determined by adding the duration of inspiration (TI) and the duration of expiration (TE). Green arrows highlight the onset of inspiration and blue arrows the onset of expiration. The onset and offset of each event occur when flow is at 0 ml/sec (red line). (E) Changes in event-related mean power (Top) and PLF (Bottom) for *Mecp2*<sup>+/y</sup> ( $n = 9$ ), *Mecp2*<sup>+/y</sup>;T158M-Tg ( $n = 9$ ), *Mecp2*<sup>T158M/y</sup> ( $n = 9$ ), and *Mecp2*<sup>T158M/y</sup>;T158M-Tg ( $n = 11$ ) Frequency bands correspond to:  $\delta$ , 2–4 Hz;  $\theta$ , 4–8 Hz;  $\alpha$ , 8–12 Hz;  $\beta$ , 12–30 Hz;  $\gamma$ low, 30–50 Hz;  $\gamma$ high, 50–90 Hz;  $\epsilon$ , 90–140 Hz. Shaded regions represent s.e.m. Top red bars represent those regions with FDR < 0.05 (permutation test). (F) Changes in event-related power (Top) and event-related PLF (Bottom) in *Mecp2*<sup>+/y</sup> and *Mecp2*<sup>+/y</sup>;T158M-Tg animals are not statistically different (two-tailed  $t$  test). Comparisons in B and C were done using 1-way ANOVA followed by Tukey's *post-hoc* test. Error bars represent mean  $\pm$  s.e.m. \* $P < 0.05$ , \*\* $P < 0.01$ .

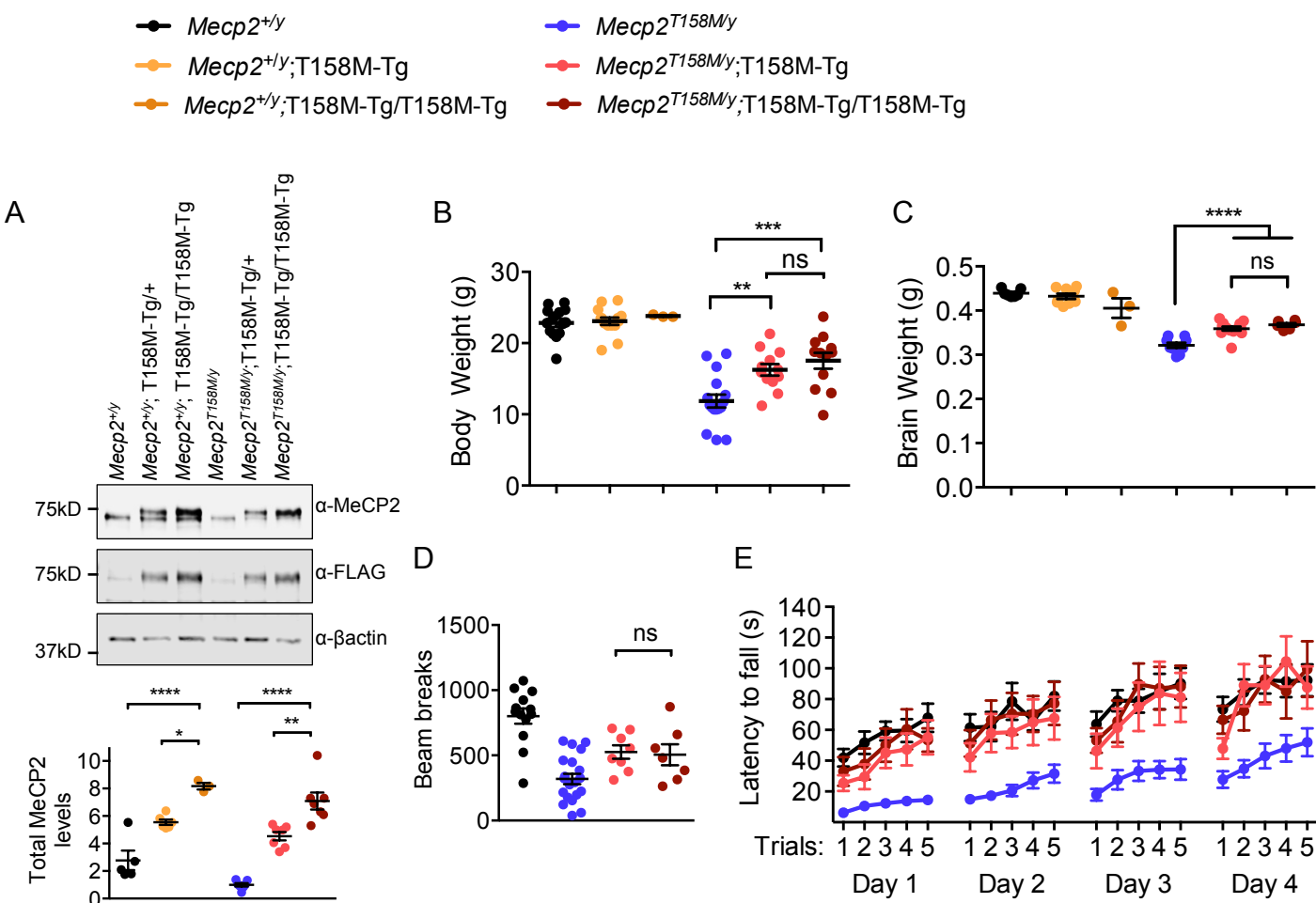


**Figure S5. Doubling the levels of MeCP2 T158M is not detrimental.** (A) Western blot analysis of MeCP2 protein levels in nuclear lysates from 12-week old male mice of the indicated genotypes. *Bottom*, quantification of total MeCP2 levels. (n = 5 for *Mecp2*<sup>+/-</sup>, n = 6 for *Mecp2*<sup>+/-</sup>;T158M-Tg, n = 3 for *Mecp2*<sup>+/-</sup>;T158M-Tg/T158M-Tg, and n = 7 for *Mecp2*<sup>T158M/y</sup>, *Mecp2*<sup>T158M/y</sup>;T158M-Tg, and *Mecp2*<sup>T158M/y</sup>;T158M-Tg/T158M-Tg). Quantification was performed using  $\beta$ -actin for normalization and values are represented as fold change relative to *Mecp2*<sup>T158M/y</sup>. Twelve-week old male *Mecp2*<sup>T158M/y</sup> animals expressing one or two copies of the MeCP2 T158M transgene have similar (B) body weight (n = 14, 14, 3, 16, 12, and 12 per genotype) and (C) brain weight (n = 7, 9, 3, 9, 13, and 6 per genotype). (D) Open field activity (n = 13 for *Mecp2*<sup>+/-</sup>, n = 21 for *Mecp2*<sup>T158M/y</sup>, n = 8 for *Mecp2*<sup>T158M/y</sup>;T158M-Tg and n = 7 for *Mecp2*<sup>T158M/y</sup>;T158M-Tg/T158M-Tg) in 10-week old males and (E) rotarod performance (n = 12, 10, 12, and 10 per genotype) in 12-week old males is similar in heterozygous *Mecp2*<sup>T158M/y</sup>;T158M-Tg and homozygous *Mecp2*<sup>T158M/y</sup>;T158M-Tg/T158M-Tg animals. Comparisons in A, B, C, and D were done using 1-way ANOVA followed by Tukey's *post-hoc* test. Comparison in E was performed using 2-way ANOVA. All bars represent  $\pm$  s.e.m. \**P*<0.05, \*\**P*<0.01, \*\*\**P*<0.001, \*\*\*\**P*<0.0001.

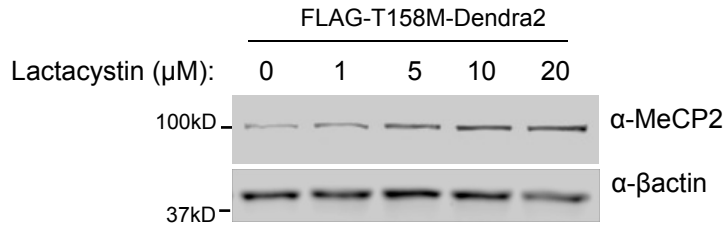


**Figure S6: The proteasome inhibitor lactacystin stabilizes the levels of MeCP2 T158M in a dose-dependent manner.** N2a cells stably expressing FLAG-T158M-Dendra2 were exposed to increasing concentrations of lactacystin and protein levels were analyzed by Western blot.  $\beta$ -actin served as loading control.